Charged-Lepton-Flavour Violation in the CMSSM in View of the Muon Anomalous Magnetic Moment

D. F. Carvalho[a], **John Ellis**[b], **M. E. Gómez**[a] and **S. Lola**[b]

a) CFIF, Departamento de Fisica, Instituto Superior Técnico, Av. Rovisco Pais,

1049-001 Lisboa, Portugal

b) CERN, CH-1211 Geneva 23, Switzerland

Abstract:

We use the BNL E821 measurement of $g_\mu - 2$, the anomalous magnetic moment of the muon, to normalize, within a supersymmetric GUT framework, constrained MSSM (CMSSM) predictions for processes that violate charged-lepton flavour conservation, including $\mu \to e\gamma$, $\mu \to e$ conversion and $K_L^0 \to \mu^\pm e^\mp$. We illustrate our analysis with two examples of lepton mass matrix textures motivated by data on neutrino oscillations. We find that $\mu \to e\gamma$ may well occur at a rate within one or two (two or three) orders of magnitude of the present experimental upper limit if $g_\mu - 2$ is within the one- (two-)standard deviation range indicated by E821. We also find that $\mu \to e$ conversion is likely to occur at rate measurable by MECO, and there is a chance that $K_L^0 \to \mu^\pm e^\mp$ may be observable in an experiment using an intense proton source.

1 Theoretical Framework

The observation of neutrino oscillations [1, 2] implies that the individual lepton numbers $L_{e,\mu,\tau}$ are violated, suggesting the appearance of processes that violate charged-lepton-number, such as $\mu \to e\gamma$, $\mu \to 3e$, $\mu \to e$ conversion on heavy nuclei [3], $\tau \to \mu\gamma$ [4] and $K_L^0 \to \mu e$ [5]. The present experimental upper limits on these processes are $\mathcal{B}(\mu \to e\gamma) < 1.2 \times 10^{-11}$ [6], $\mathcal{B}(\mu^+ \to e^+e^+e^-) < 1.0 \times 10^{-12}$ [7], $\mathcal{B}(\mu^- Ti \to e^- Ti) < 6.1 \times 10^{-13}$ [8], $\mathcal{B}(\tau \to \mu\gamma) < 1.1 \times 10^{-6}$ [9] and $\mathcal{B}(K_L^0 \to \mu^\pm e^\mp) < 4.7 \times 10^{-12}$ [10]. On the other hand, in minimal GUT models where the small neutrino masses are generated by the see-saw mechanism with massive singlet neutrinos ν_R, and there are no new lighter particles, the amplitudes for charged-lepton-flavour violation are proportional to inverse powers of the heavy singlet neutrino mass M_{ν_R}, and the rates for rare decays are extremely suppressed [11].

However, the observation of an apparent discrepancy between the measured value of the anomalous magnetic moment of the muon, $a_\mu \equiv (g_\mu - 2)/2$, and the value predicted in the Standard Model [12] suggests the appearance of new physics at the TeV scale in the lepton sector, with superseymmetry being one of the favoured options [13, 14]. Moreover, there is a striking resemblance between the effective operators that generate $\mu \to e\gamma$ and δa_μ:

$$\mathcal{L}_{eff} = e \frac{m_{\ell_j}}{2} \bar{\ell}_i \sigma_{\mu\nu} F^{\mu\nu} (A_M^{L,ij} P_L + A_M^{R,ij} P_R) \ell_j \tag{1}$$

resulting in

$$\mathrm{Br}(\mu \to e\gamma) = \frac{48\pi^3 \alpha}{G_F^2} (|A_M^{L,12}|^2 + |A_M^{R,12}|^2) \tag{2}$$

and

$$\delta a_\mu = \frac{m_\mu^2}{2} (A_M^{L,22} + A_M^{R,22}). \tag{3}$$

Hence, if these quantities are dominated by either the A_M^L or the A_M^R, there is a direct relation between them:

$$\mathcal{B}(\mu \to e\gamma) = \frac{192\pi^3 \alpha}{G_F^2 m_\mu^4} \times (\delta a_\mu)^2 \times \epsilon^2, \tag{4}$$

where the lepton mixing factor $\epsilon \equiv A_M^{L/R,12}/A_M^{L/R,22}$. We see explicitly from (4) that the apparent measurement of δa_μ enables the rate for $\mu \to e\gamma$ to be predicted, in the context of any model of lepton flavour violation motivated by the observations of neutrino oscillations which is able to predict ϵ.

One example of a theory where this connection can be made is supersymmetry [15, 16]. In a supersymmetric model, the amplitudes for processes violating charged lepton number are suppressed by inverse powers of the supersymmetry-breaking scale, which is thought to be at most 1 TeV. In particular, in the presence of $\tilde{\mu}$-$\tilde{e}$ ($\tilde{\nu}_\mu$-$\tilde{\nu}_e$) mixing, the

2

diagrams of Fig. 1 are generated, which are isomorphic to the corresponding flavour-conserving diagrams contributing to δa_μ. If the dominant supersymmetric contribution to $g_\mu - 2$ comes from the chargino-sneutrino diagram Fig. 1(b) involving left-handed leptons, one expects the chargino diagrams also to dominate $\mu \to e\gamma$ *. Taking the BNL E821 measurement of the muon anomalous magnetic moment [12] at its face value fixes the overall mass scale of the sparticles circulating in the loops in Fig. 1, and a supersymmetric GUT model of ν_μ-ν_e mixing can be used to calculate the amount of $\tilde{\mu}$-$\tilde{e}$ and $\tilde{\nu}_\mu$-$\tilde{\nu}_e$ mixing, i.e., the factor ϵ in (4), enabling the rate for $\mu \to e\gamma$ to be predicted.
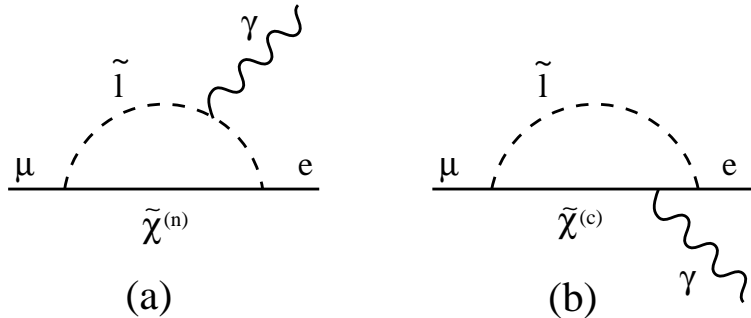

Figure 1: *Generic Feynman diagrams for $\mu \to e\gamma$ decay: $\tilde{l}$ represents a charged slepton (a) or sneutrino (b), and $\tilde{\chi}^{(n)}$ and $\tilde{\chi}^{(c)}$ represent neutralinos and charginos respectively.*

Connections to other processes violating charged-lepton flavour, such as $\mu \to 3e$ and $\mu \to e$ conversion on nuclei, can be made in a similar way, though less directly. Among these processes, $\mu \to e$ conversion is particularly promising, since the present experimental sensitivity may be improved by several orders of magnitude in future experiments such as MECO [17] and PRISM [3]. These processes receive important contributions from photon and Z 'penguin' diagrams, which are related to those for $\mu \to e\gamma$ via a virtual gauge boson coupling to an e^+e^- or a quark-antiquark pair, but also from box diagrams and their supersymmetric analogues. The dominant photonic contribution yields [3] $\mathcal{B}(\mu Ti \to eTi) \approx 5.6 \times 10^{-3} \mathcal{B}(\mu \to e\gamma)$, but this ratio may receive substantial corrections from subdominant contributions, which we take into account in our calculations. Finally, we also mention the possibility in supersymmetric theories of observing charged-lepton-flavour violation in $K_L^0 \to \mu e$ decay [5]. This involves the mixing of squarks as well as that of sleptons, thus providing additional information. The rate is small in the CMSSM with right-handed neutrinos, but might be observable using a future intense proton source, if $\tan\beta$ is large †.

In all these processes, the magnitudes of the rates depend on the masses and mixings of sparticles. Excessive rates for charged-lepton-flavour violation are generically pre-

---

*When the right-handed sleptons also contribute significantly to the lepton-flavour-violating masses, the neutralino–slepton diagrams of Fig. 1(a) also contribute to $\mu \to e\gamma$, modifying the correlation between $\mu \to e\gamma$ and $g_\mu - 2$.

†Larger rates are also possible in supersymmetric models with broken R parity [5], a possibility not considered in this paper.

dicted in models with non-universal scalar masses at the GUT scale. Thus we consider constrained MSSM (CMSSM) models that respect this universality, such as minimal supergravity (mSUGRA) [18], gauge-mediated supersymmetry [19] and no-scale models [20]. In such models, even though there are no off-diagonal contributions to the sfermion mass matrix at M_{GUT}, renormalization effects due to lepton Dirac Yukawa couplings within the Minimal Supersymmetric Standard Model (MSSM) with massive neutrinos spoil this diagonal form [21], making these processes observable.

In this paper, we calculate these quantum corrections in the context of the most natural mechanism for obtaining sub-eV neutrino masses, namely the see-saw mechanism [22]. This involves Dirac neutrino masses m_{ν_D} of the same order as the charged-lepton and quark masses, and heavy Majorana masses M_{ν_R}, leading to a light effective neutrino mass matrix:

$$m_{eff} = m_{\nu_D} \cdot (M_{\nu_R})^{-1} \cdot m_{\nu_D}^T. \tag{5}$$

Neutrino-flavour mixing may then occur through either the Dirac and/or the Majorana mass matrices, which may also feed flavour violation through to the charged leptons.

In general, the Dirac neutrino and charged-lepton Yukawa couplings, λ_{ν_D} and λ_ℓ respectively, cannot be diagonalized simultaneously. Since both these sets of lepton Yukawa couplings appear in the renormalization-group equations, the lepton Yukawa matrices and the slepton mass matrices cannot be diagonalized simultaneously at low energies, either. In the basis where λ_ℓ and m_ℓ are diagonal, the slepton-mass matrix acquires non-diagonal contributions from renormalization at scales below M_{GUT}, of the form:

$$\delta m_{\tilde{\ell}}^2 \propto \frac{1}{16\pi^2}(3 + a^2) \ln \frac{M_{GUT}}{M_N} \lambda_{\nu_D}^\dagger \lambda_{\nu_D} m_{3/2}^2, \tag{6}$$

where a is related to the trilinear mass parameter: $A_\ell \equiv a m_0$, where m_0 is the common assumed value of the scalar masses at the GUT scale.

Different oscillation scenarios for the atmospheric and solar neutrino deficits [23], e.g., those with small/large neutrino mixing angles and with eV or much lighter neutrinos, predict in general different rates for lepton-flavour violation. Typically, the larger the ν_μ-ν_e mixing and the larger the neutrino mass scale, the larger the rates. Thus, models of degenerate neutrinos with bimaximal mixing lead to significantly larger effects than, for instance, hierarchical neutrinos with a small vacuum mixing angle. Just-so vacuum solutions to the solar neutrino deficit with $\delta m^2 \approx 10^{-10}$ eV^2 typically predict small rates if the neutrino masses are hierarchical, even if the (1-2) mixing angle is large.

2   Sample Models of Neutrino Masses and Mixing

In order to illustrate our estimates of the expected effects, we calculate the rates for rare processes violating charged-lepton number in representatives of two different types of models, one with small and one with large μ-e mixing. The first model (A) is based on Abelian flavour symmetries and symmetric fermion mass matrices [24], and

leads to the following pattern of charged-lepton masses m_ℓ, neutrino Dirac masses m_{ν_D}, charged-lepton mixing V_ℓ and Dirac mixing V_{ν_D} [25]:

$$
m_\ell \propto \begin{pmatrix} \bar\epsilon^7 & \bar\epsilon^3 & \bar\epsilon^{7/2} \\ \bar\epsilon^3 & \bar\epsilon & \bar\epsilon^{1/2} \\ \bar\epsilon^{7/2} & \bar\epsilon^{1/2} & 1 \end{pmatrix}, m_{\nu_D} \propto \begin{pmatrix} \bar\epsilon^{14} & \bar\epsilon^6 & \bar\epsilon^7 \\ \bar\epsilon^6 & \bar\epsilon^2 & \bar\epsilon \\ \bar\epsilon^7 & \bar\epsilon & 1 \end{pmatrix},
\tag{7}
$$

$$
V_\ell = \begin{pmatrix} 1 & \bar\epsilon^2 & -\bar\epsilon^{7/2} \\ -\bar\epsilon^2 & 1 & \bar\epsilon^{1/2} \\ \bar\epsilon^{7/2} & -\bar\epsilon^{1/2} & 1 \end{pmatrix}, V_{\nu_D} = \begin{pmatrix} 1 & \bar\epsilon^4 & -\bar\epsilon^7 \\ -\bar\epsilon^4 & 1 & \bar\epsilon \\ \bar\epsilon^7 & -\bar\epsilon & 1 \end{pmatrix},
\tag{8}
$$

where $\bar\epsilon$ is a (small) expansion parameter related to the Abelian symmetry-breaking scale. In this model, even a charged-lepton matrix with large (2-3) mixing always predicts small $\mu - e$ mixing, as a result of fixing the charged-lepton mass hierarchies [25].

As a second possible model (B), we discuss the case of bimaximal mixing appearing in [26]. In the basis where the charged-lepton mass matrix is diagonal, the neutrino mixing matrix is:

$$
V_{\nu_D} = \begin{pmatrix} \frac{1}{\sqrt{2}} & -\frac{1}{\sqrt{2}} & 0 \\ \frac{1}{2} & \frac{1}{2} & -\frac{1}{\sqrt{2}} \\ \frac{1}{2} & \frac{1}{2} & \frac{1}{\sqrt{2}} \end{pmatrix}
\tag{9}
$$

corresponding to a neutrino mass matrix of the form

$$
m_{eff} = m \left[\begin{pmatrix} 0 & 0 & 0 \\ 0 & 1 & -1 \\ 0 & -1 & 1 \end{pmatrix} + \begin{pmatrix} 2\epsilon_B & \delta & \delta \\ \delta & \epsilon_B & \epsilon_B \\ \delta & \epsilon_B & \epsilon_B \end{pmatrix} \right],
\tag{10}
$$

where the mass parameters in this texture are related to the mass eigenvalues by

$$
\begin{aligned}
m &= m_3/2, & \text{(11)} \\
\epsilon_B &= (m_2 + m_1)/4m, & \text{(12)} \\
\delta &= \sqrt{2}\,(m_1 - m_2)/4m. & \text{(13)}
\end{aligned}
$$

In our analysis we assume hierarchical neutrinos, but the case of degenerate neutrinos can be treated similarly. This would lead to different predictions, since the neutrino mass scales change, typically with larger rates for charged-lepton-flavour violation. Hence our results for model (B) are quite conservative.

3   Supersymmetric Calculations

We have calculated the rates for processes violating charged lepton number in both frameworks, including complete sets of one-loop sparticle diagrams. We parametrize the universal soft supersymmetry-breaking masses by the GUT-scale parameters m_0 and $m_{1/2}$, for sfermions and gauginos respectively, and use the renormalization-group

equations of the CMSSM to calculate the low-energy sparticle masses [21]. Other relevant free parameters of the MSSM are the trilinear coupling A, the sign of the Higgs mixing parameter μ, and the ratio of Higgs vev's, $\tan\beta$. Here we consider only $\mu > 0$, since this is the sign favoured by $g_\mu - 2$. The physical charged-slepton masses are found by numerical diagonalization of the following matrix:

$$\tilde{m}_\ell^2 = \begin{pmatrix} m_{LL}^2 & m_{LR}^2 \\ m_{RL}^2 & m_{RR}^2 \end{pmatrix} \tag{14}$$

where all the entries are 3×3 matrices in flavour space. Using the superfield basis where the Yukawa coupling matrix λ_ℓ is diagonal, we can write:

$$m_{LL}^2 = (m_{\tilde{\ell}}^\delta)^2 + \delta m_{\nu_D}^2 + m_\ell^2 - M_Z^2(\frac{1}{2} - sin^2\theta_W)\cos 2\beta \tag{15}$$

$$m_{RR}^2 = (m_{\tilde{e}_R}^\delta)^2 + m_\ell^2 - M_Z^2\sin^2\theta_W\cos 2\beta \tag{16}$$

$$m_{RL}^2 = (A_e^\delta + \delta A_e - \mu\tan\beta)m_\ell \tag{17}$$

$$m_{LR}^2 = m_{RL}^{2\dagger} \tag{18}$$

where $(m_{\tilde{\ell}}^\delta)^2, (m_{\tilde{e}_R}^\delta)^2$ and A_e^δ denote the diagonal contributions to the corresponding matrices, obtained by numerical integration of the renormalization-group equations, and $\delta m_{\nu_D}^2$ and δA_l denote the off-diagonal terms that appear because λ_{ν_D} and λ_ℓ may not be diagonalized simultaneously - see (6). Analogously, for sneutrinos we have

$$m_{\tilde{\nu}}^2 = (m_{\tilde{\ell}}^\delta)^2 + \delta m_{\nu_D}^2 + \frac{1}{2}M_Z^2 cos2\beta \tag{19}$$

The mixing parameter ϵ in (4) is given in terms of the parameters of this matrix. In the simplified case where the lepton-number-violating mass terms are in the $\tilde{\ell}_L$ sector, so that the chargino-sneutrino diagram dominates both $g_\mu - 2$ and $\mu \to e\gamma$, assuming that the sparticle masses have (approximately) a common value $\tilde{m}$, and making a naive mass-insertion approximation, one would find

$$\epsilon \approx \frac{(m_{\tilde{\nu}}^2)_{12}}{\tilde{m}^2}, \tag{20}$$

but this is only indicative, and we use complete formulae in our results below.

We start by fixing the elements of the Yukawa coupling matrices at the GUT scale to be consistent with the experimental values of the fermion masses and the absolute values of the CKM matrix elements [4]. This is done by choosing appropriate coefficients of order one in the entries of the lepton matrices. In the notation of [4], we choose for model (A):

$$C_{12} = 0.77, \quad C_{23} = 0.79, \tag{21}$$

and for model (B):

$$C_{12} = 2.75, \quad C_{23} = 1.13, \tag{22}$$

with the unspecified coefficients taken as unity. These coefficients do not change significantly for the two values of $\tan\beta$ considered in the present work.

We then use the full Yukawa coupling matrices in the renormalization-group equations, including the effects of λ_{ν_D} on the CMMSM parameters at the see-saw mass scale [27]. We have checked that our results using the full matricial forms for the Yukawa couplings do not differ significantly from the common approach of considering diagonal Yukawa matrices and neglecting the lighter generations. We check our results by constructing the slepton mass matrices in the superfield base where the λ_ℓ are diagonal and inserting the non–diagonal elements induced by the presence of λ_{ν_D} on the renormalization-group equations between the GUT and see-saw mass scales. Finally, we use the full matricial forms for all the parameters which appear in the vertices in the diagrams of Fig. 1, and the results of [28] to calculate the rates for $\mu \to e\gamma$ and $\mu \to e$ conversion, and those of [5] to calculate the rate for $K_L^0 \to \mu e$.

4   Constraints on the CMSSM

We display in the remaining figures the $(m_0, m_{1/2})$ planes in the CMSSM for $\tan\beta = 10, 30$, assuming $\mu > 0$ as suggested by the sign of δa_μ, and $A_0 = 0$. The experimental constraints on the CMSSM are taken from [29, 13], where further details of their implementation can be found. We note in particular that the following choices are used here for the pole mass of the top quark: $m_t = 175$ GeV, and for the running mass of the bottom quark: $m_b(m_b)_{SM}^{\overline{MS}} = 4.25$ GeV. We combine the constraints given in [29, 13] with the contours suggested by the neutrino mass textures introduced above for $\mathcal{B}(\mu \to e\gamma)$ in Fig. 2, for $\mathcal{B}(\mu^- Ti \to e^- Ti)$ in Fig. 3, and for $\mathcal{B}(K_L^0 \to \mu^\pm e^\mp)$ in Fig. 4.

The dark (brick-red) shaded regions in the $(m_0, m_{1/2})$ planes in these figures are excluded [29] because the lightest supersymmetric particle is the lighter $\tilde{\tau}$, which is disallowed by the astrophysical requirement that cold dark matter be electrically neutral. The light (turquoise) shaded regions are those where the LSP is the lightest neutralino χ, and its cosmological relic density $\Omega_\chi h^2$ lies in the favoured range $0.1 \leq \Omega_\chi h^2 \leq 0.3$ [29]. Lower values of $\Omega_\chi h^2$ would be possible if there are other sources of cold dark matter, whereas larger values of $\Omega_\chi h^2$, which occur generically at larger values of $m_{1/2}$ and m_0, are excluded by cosmology.

We display as (red) dash-dotted lines mass contours for the lightest CMSSM Higgs boson: $m_h = 113, 117$ GeV, as calculated in [29]. This range corresponds roughly to values of $m_{1/2}$ and m_0 that are compatible, within theoretical errors, with the LEP Higgs 'signal' at $m_H = 115^{+1.3}_{-0.7}$ GeV [30], for our default choices of A_0, m_t and $m_b(m_b)_{SM}^{\overline{MS}}$. There is good overall consistency between m_h and the other constraints for $10 \lesssim \tan\beta \lesssim 55$, but we do not insist on the range 113 GeV $\leq m_h \leq 117$ GeV, in view of the theoretical uncertainties and because the LEP Higgs 'signal' might turn out to be a false alarm, in which case m_h could be larger.

The medium dark (green) shaded regions in panels (b) and (d) are excluded by our implementation of the $b \to s\gamma$ constraint. As described in [29], we use the latest NLO QCD calculations for large $\tan\beta$ and allow values of $m_{1/2}$ and m_0 that, after including the expected theoretical errors due to the scale choice and model dependences, may fall

within the 95% confidence level range $2.33 \times 10^{-4} < \mathcal{B}(b \to s < \gamma) < 4.15 \times 10^{-4}$. In the panels (a) and (c) of the figures, for $\tan\beta = 10$, there is no relevant constraint from $b \to s\gamma$, and we display as a dashed line the LEP lower limit $m_{\chi^\pm} > 104$ GeV. There is a similar constraint in the panels (b) and (d), for $\tan\beta = 30$, which is omitted for clarity.

To complement our summary of [29], we note that the regions allowed by the E821 measurement of a_μ at the 2-σ level [12] are shown in the figures as light (pink) shaded regions with solid black line boundaries [13]. Also shown as black dashed lines are the regions favoured by a_μ at the 1-σ level. We emphasize the impressive consistency between the constraints from a_μ, m_h, $b \to s\gamma$ and cosmology for $\tan\beta \gtrsim 10$. As discussed in [13], combining all the other constraints with the 1-σ range for a_μ, one finds quite small allowed regions of the $(m_{1/2}, m_0)$ plane centred on: $\sim (250, 100)$ GeV for $\tan\beta = 10$ (see panels (a) and (c)) and $\sim (350, 170)$ GeV for $\tan\beta = 30$ (see panels (b) and (d)).

5 Results for Processes Violating Charged-Lepton Number

Fig. 2 displays the predictions for $\mathcal{B}(\mu \to e\gamma)$ in texture (A) (panels (a) and (b)) and texture (B) (panels (c) and (d)). We see that texture (A) generically predicts that $\mathcal{B}(\mu \to e\gamma)$ should occur *within one or two (two or three) orders of magnitude of the present experimental upper limit* if a_μ lies within the 1(2)-σ range suggested by E821 [12]. Within this model, the experimental upper limit on $\mathcal{B}(\mu \to e\gamma) < 1.2 \times 10^{-11}$ excludes a domain of the $(m_{1/2}, m_0)$ plane, close to the origin, that may be compared to that excluded by slepton searches at LEP. When $\tan\beta \sim 10$, it also has a similar effect to that of the upper limit on the supersymmetric contribution to $g_\mu - 2$. For larger $\tan\beta \sim 30$, the constraint due to the present upper limit on $\mathcal{B}(\mu \to e\gamma)$ is intermediate between the $g_\mu - 2$ and $b \to s\gamma$ constraints. In model (B), we find values of $\mathcal{B}(\mu \to e\gamma)$ that are characteristically about an order of magnitude smaller than in model (A) in the parameter region allowed by cosmology [29] and $g_\mu - 2$ [13].

As already mentioned, the rate for $\mu^- Ti \to e^- Ti$ conversion is linked to that for $\mathcal{B}(\mu \to e\gamma)$, with a proportionality coefficient $\sim 5.6 \times 10^{-3}$ if $\mu^- Ti \to e^- Ti$ is dominated by photon exchange. However, this is not necessarily the case, since Z^0 exchange and box diagrams may also contribute, rendering the ratio $\mathcal{B}(\mu^- Ti \to e^- Ti)/\mathcal{B}(\mu \to e\gamma)$ non-universal. Accordingly, we plot in Fig. 3 the predictions of texture (A) (panels (a) and (b)) and texture (B) (panels (c) and (d) for $\mathcal{B}(\mu^- Ti \to e^- Ti)$. We see that there are large domains of the $(m_{1/2}, m_0)$ plane where these textures suggest that $\mathcal{B}(\mu^- Ti \to e^- Ti) > 10^{-16}$, which is the sensitivity of the proposed MECO experiment [17, 3]. In model (A), these include all the regions allowed by $g_\mu - 2$ at the 2-σ level, and, in model (B), most of the allowed region. *We infer that the physics interest of this proposal is greatly enhanced by the recent result on $g_\mu - 2$ from E821 [12].*
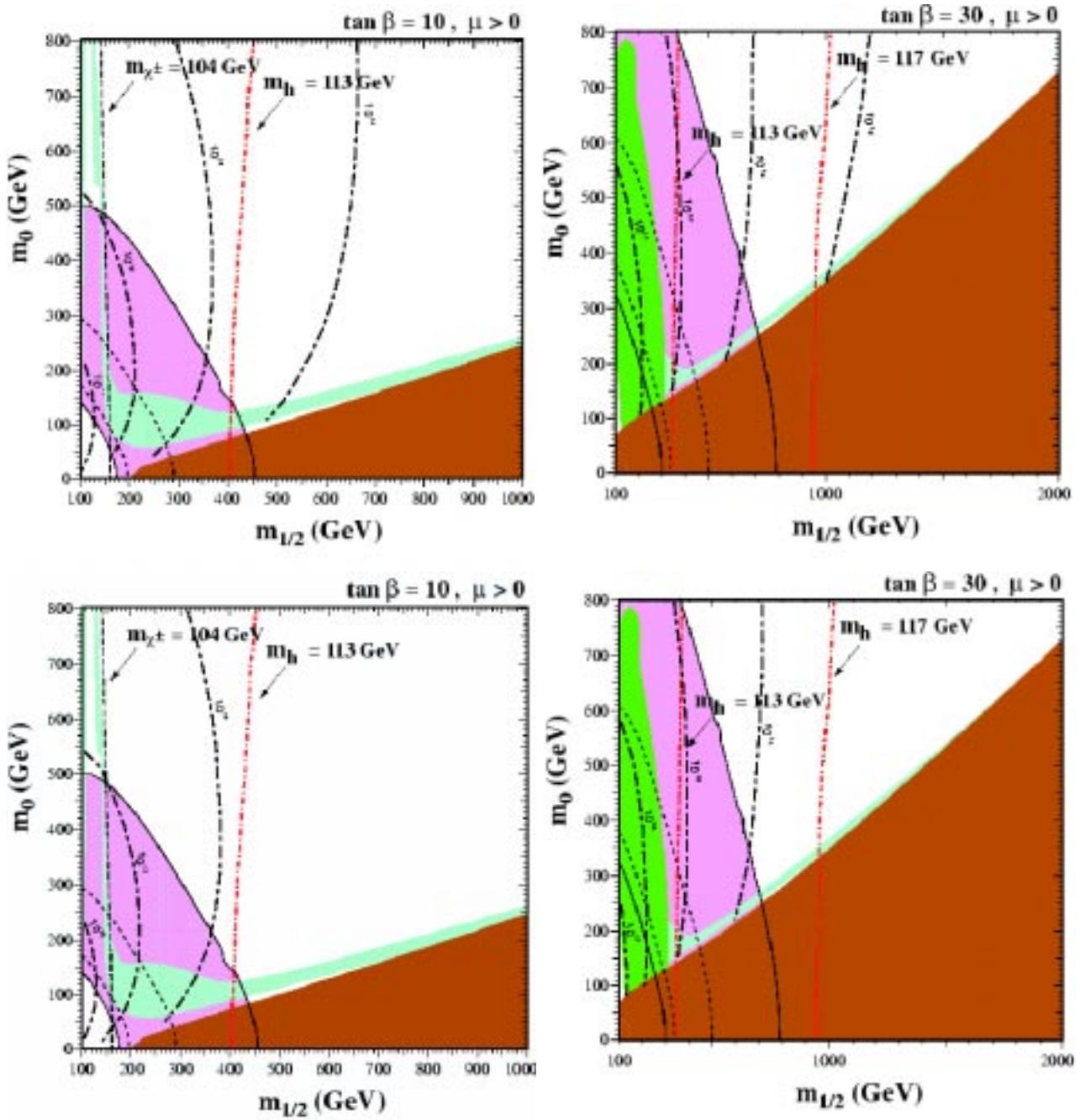
Figure 2: *The contours* $\mathcal{B}(\mu \to e\gamma) = 10^{-11}, 10^{-12}, 10^{-13}$ *and* 10^{-14} *in (a, b) texture (A) and (c, d) texture (B) are shown as dash-dotted black lines in the* $(m_{1/2}, m_0)$ *planes for* $\mu > 0$ *and* $\tan\beta = $ *(a, c) 10 and (b, d) 30. Other constraints in these planes are taken from [29], assuming* $A_0 = 0, m_t = 175$ *GeV and* $m_b(m_b)_{SM}^{\overline{MS}} = 4.25$ *GeV. The regions allowed by the E821 measurement of* a_μ *at the 2-σ level [12] are shaded (pink) and bounded by solid black lines, with dashed lines indicating the 1-σ ranges [13]. The dark (brick-red) shaded regions are excluded because the LSP is the charged* $\tilde{\tau}_1$, *and the light (turquoise) shaded regions are those with* $0.1 \leq \Omega_\chi h^2 \leq 0.3$ *that are preferred by cosmology. We show the contours* $m_h = 113, 117$ *GeV, and in panels (a, c) the contour* $m_{\chi^\pm} = 104$ *GeV. The medium (dark green) shaded regions are excluded by* $b \to s\gamma$.
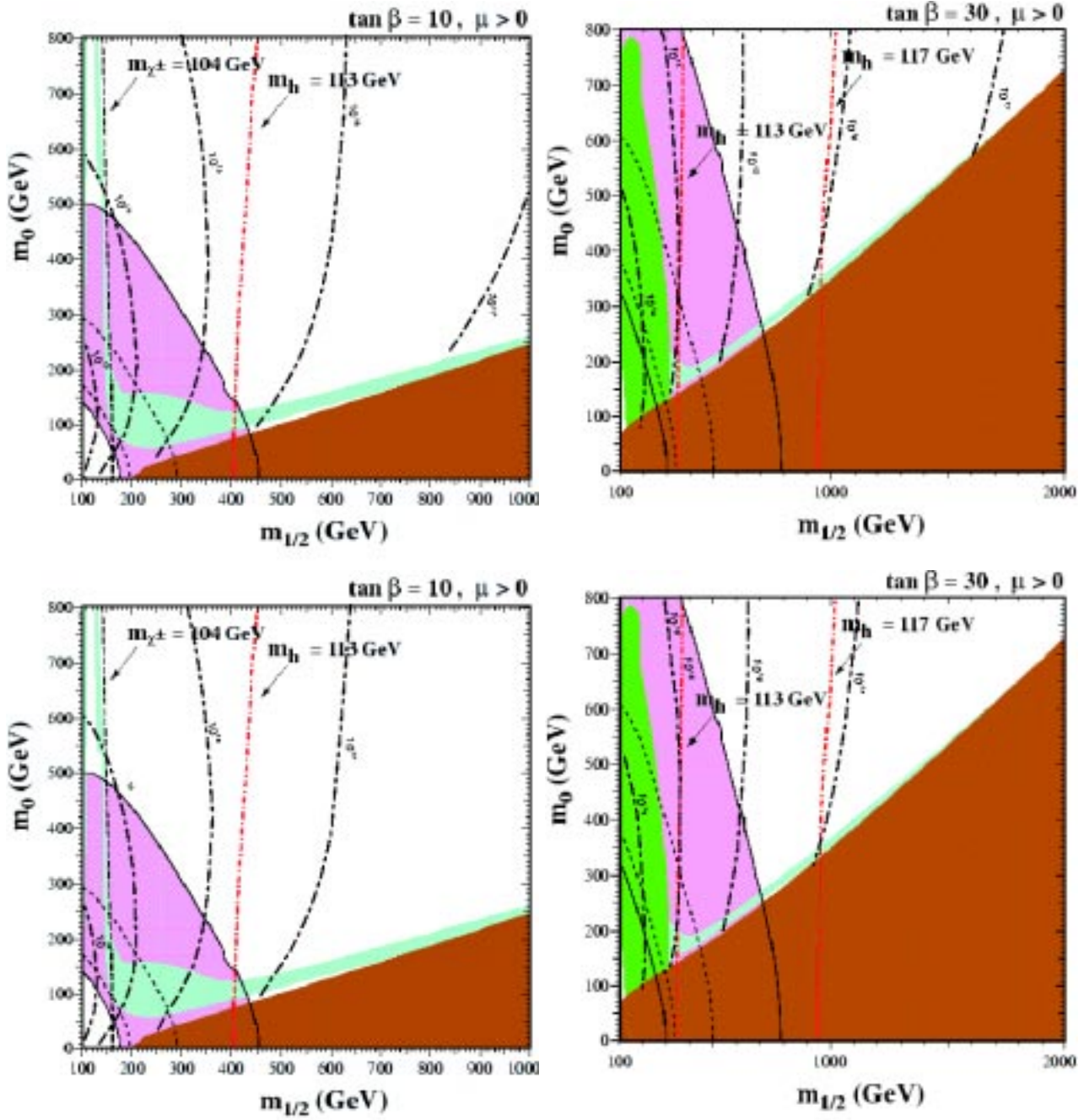
Figure 3: *The contours* $\mathcal{B}(\mu^- Ti \rightarrow e^- Ti) = 10^{-13}, 10^{-14}, 10^{-15}, 10^{-16}$ *and* 10^{-17} *in (a, b) texture (A) and (c, d) texture (B) are shown as dash-dotted black lines in the* $(m_{1/2}, m_0)$ *planes for* $\mu > 0$ *and* $\tan \beta = (a, c)$ *10 and (b, d) 30. Other constraints in these planes are taken from [29, 13], as described in the caption of Fig. 2.*

10

Finally, we plot in Fig. 4 the corresponding model predictions for $\mathcal{B}(K_L^0 \to \mu^\pm e^\mp)$. This process is very interesting [5], because it combines flavour violation in the quark and lepton sectors. For this same reason, one expects rather small values of $\mathcal{B}(K_L^0 \to \mu^\pm e^\mp)$, far below the present experimental upper limit. However, again for this same reason, there is clearly even more uncertainty in the predictions for $\mathcal{B}(K_L^0 \to \mu^\pm e^\mp)$ than there was already for $\mathcal{B}(\mu \to e\gamma)$ and $\mathcal{B}(\mu^- Ti \to e^- Ti)$. The sensitivity to the lepton mass texture is seen clearly by comparing panels (a, b) and (c, d) of Fig. 4. Nevertheless, we note that $\mathcal{B}(K_L^0 \to \mu^\pm e^\mp) > 10^{-18}$ in a significant fraction of the parameter region favoured by $g_\mu - 2$ at the one-σ level. Thus, we think that *this process is of potential interest* at an intense proton source.

6   Conclusions

We have argued in this paper that the BNL E821 measurement of $g_\mu - 2$ [12], taken at face value, may be used to normalize predictions for the charged-lepton-number-violating processes $\mu \to e\gamma$, $\mu \to e$ conversion and $K_L^0 \to \mu^\pm e^\mp$, within a supersymmetric GUT framework. We have illustrated our argument with a couple of specific textures for fermion masses that are consistent with the data on neutrino oscillations. In these examples, we find that $\mu \to e\gamma$ decay may appear at a rate within one or two (two or three) orders of magnitude of the present experimental upper limit if $g_\mu - 2$ lies within its present one- (two-)σ range. These models also make us optimistic that $\mu \to e$ conversion on heavy nuclei may be accessible to the next round of experiments [17, 3]. The prospects for observing $K_L^0 \to \mu^\pm e^\mp$ decay are not so rosy, but this decay might also be accessible to some future round of experiments with an intense proton source.

The discovery of neutrino oscillations has been a major breakthrough in flavour physics. If confirmed, the deviation of $g_\mu - 2$ from the SM prediction would be a breakthrough towards new physics at the TeV scale. Their combination suggests not only that the conservation of charged lepton number is not sacred, but also that its violation may soon be observable. If so, this would be an invaluable new window on the physics of lepton flavour, as well as on physics at the TeV scale. It would provide a bridge between neutrino oscillations and accelerator physics, as well as yield novel information on lepton mixing.

We encourage strongly the most sensitive possible experiments to probe the violation of charged lepton number.
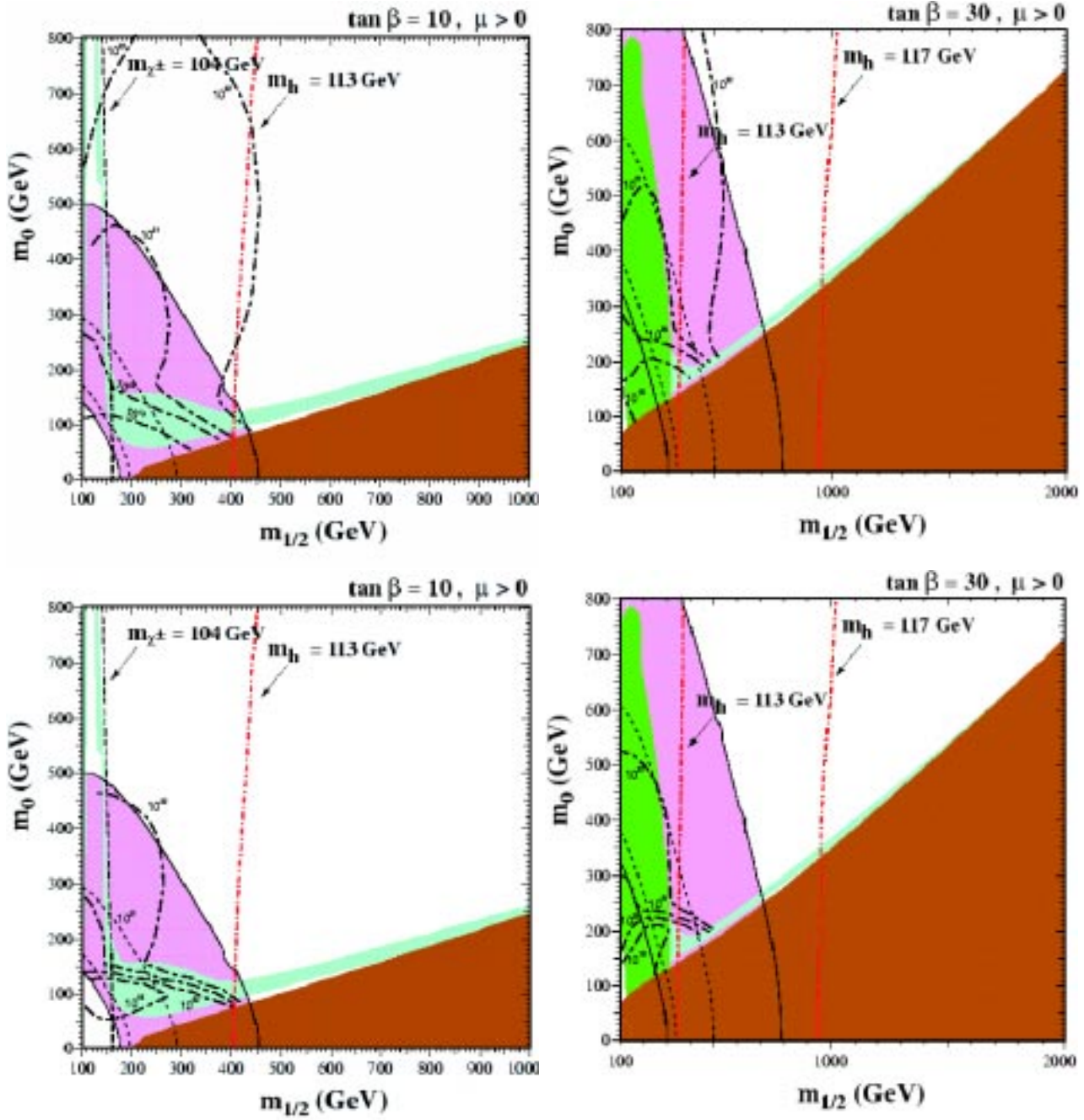
Acknowledgements

Figure 4: *The contours $\mathcal{B}(K_L^0 \to \mu^\pm e^\mp) = 10^{-18}, 10^{-20}, 10^{-21}$ and 10^{-22} in (a, b) texture (A) and (c, d) texture (B) are shown as dash-dotted black lines in the $(m_{1/2}, m_0)$ planes for $\mu > 0$ and $\tan\beta = $ (a, c) 10 and (b, d) 30. Other constraints in these planes are taken from [29, 13], as described in the text.*

discussions related to this analysis.

References

[1] S. Fukuda *et al.*, Super-Kamiokande Collaboration, hep-ex/0103032 and hep-ex/0103033; and references therein.

[2] Y. Fukuda *et al.*, Super-Kamiokande Collaboration, Phys. Lett. B433 (1998) 9; Phys. Lett. B436 (1998) 33; Phys. Rev. Lett. 81 (1998) 1562.

[3] For a recent review, see: Y. Kuno and Y. Okada, hep-ph/9909265.

[4] M. E. Gómez, G. Leontaris, S. Lola and J. Vergados, Phys. Rev. D59 (1999) 116009; J. Ellis, M. E. Gómez, G. Leontaris, S. Lola and D. V. Nanopoulos, Eur. Phys. J. C14 (2000) 319; and references therein.

[5] A. Belyaev, M. Chizhov, A. Dorokhov, J. Ellis, M. E. Gómez and S. Lola, hep-ph/0008276; and references therein.

[6] M. L. Brooks *et al.*, MEGA Collaboration, Phys. rev. Lett. 83 (1999) 1521.

[7] U. Bellgardt *et al.*, Nucl. Phys. B229 (1988) 1.

[8] P. Wintz, *Proceedings of the First International Symposium on Lepton and Baryon Number Violation*, eds. H.V. Klapdor-Kleingrothaus and I.V. Krivosheina (Institute of Physics, Bristol, 1998), p.534.

[9] S. Ahmed *et al.*, CLEO Collaboration, Phys. Rev. D61 (2000) 071101.

[10] D. Ambrose *et al.*, BNL E871 Collaboration, Phys. Rev. Lett. 81 (1998) 5734.

[11] S. T. Petcov, Yad. Phys. 25 (1977) 641 and Sov. J. Nucl. Phys. 25 (1977) 340; S. M. Bilenki, S. T. Petcov and B. Pontecorvo, Phys. Lett. B67 (1977) 309.

[12] H. N. Brown *et al.*, BNL E821 Collaboration, hep-ex/0102017.

[13] J. Ellis, D. V. Nanopoulos and K. A. Olive, hep-ph/0102331.

[14] For other supersymmetric analyses of the E821 result, see: L. Everett, G. L. Kane, S. Rigolin and L. Wang, hep-ph/0102145; J. L. Feng and K. T. Matchev, hep-ph/0102146; E. A. Baltz and P. Gondolo, hep-ph/0102147; U. Chattopadhyay and P. Nath, hep-ph/0102157; S. Komine, T. Moroi and M. Yamaguchi, hep-ph/0102204; R. Arnowitt, B. Dutta, B. Hu and Y. Santoso, hep-ph/0102344; T. Kobayashi and H. Terao, hep-ph/0103028; K. Choi, K. Hwang, S. K. Kang and K. Y. Lee, hep-ph/0103048; S. P. Martin and J. D. Wells, hep-ph/0103067; S. Komine, T. Moroi and M. Yamaguchi, hep-ph/0103182; K. Cheung, C. H. Chou and O. C. W. Kong, hep-ph/0103183; S. Baek, P. Ko and H. S. Lee, hep-ph/0103218.

[15] J. Hisano and K. Tobe, hep-ph/0102315.

[16] For other analyses of charged-lepton-flavour violation in view of the E821 result, see: T. Huang, Z. H. Lin, L. Y. Shan and X. Zhang, hep-ph/0102193; E. Ma and M. Raidal, hep-ph/0102255; X. Calmet, H. Fritzsch and D. Holtmannspotter, hep-ph/0103012; S. K. Kang and K. Y. Lee, hep-ph/0103064; M. Raidal, hep-ph/0103224.

[17] M. Bachmann *et al.*, MECO Collaboration, BNL Research Proposal E940 (1997).

[18] H. P. Nilles, Phys. Rept 110 (1984) 1 and references therein.

[19] M. Dine and A. Nelson, Phys. Rev. D48 (1993) 1277; S. Dimopoulos, S. Thomas and J.D. Wells, Nucl. Phys. B488 (1997) 39; G. Giudice and R. Rattazzi, Phys. Rept. 322 (1999) 419 and references therein.

[20] J. Ellis, C. Kounnas and D. V. Nanopoulos, Nucl. Phys. B247 (1984) 373; J. Ellis, A. B. Lahanas, D. V. Nanopoulos and K. Tamvakis, Phys. Lett. B134 (1984) 429.

[21] F. Borzumati and A. Masiero, Phys. Rev. Lett. 57 (1986) 961; J. Hisano, T. Moroi, K. Tobe and M. Yamaguchi, Phys. Lett. B391 (1997) 341, [Erratum - ibid. B397 (1997) 357]; S.F. King and M. Oliveira, Phys. Rev. D60 (1999) 035003.

[22] M. Gell-Mann, P. Ramond and R. Slansky, *Proceedings of the Stony Brook Supergravity Workshop*, New York, 1979, eds. P. Van Nieuwenhuizen and D. Freedman (North-Holland, Amsterdam).

[23] For a review, see G. Altarelli and F. Feruglio, Phys. Rept. 320 (1999) 295, and references therein.

[24] L. Ibáñez and G. G. Ross, Phys. Lett. B332 (1994) 100.

[25] S. Lola and G. G. Ross, Nucl. Phys. B553 (1999) 81; G. K. Leontaris, S. Lola and G. G. Ross, Nucl. Phys. B454 (1995) 25.

[26] V. Barger, S. Pakvasa, T. J. Weiler and K. Whisnant, Phys. Lett. B437 (1998) 107.

[27] A. Casas and A. Ibarra, hep-ph/0103065.

[28] J. Hisano, T. Moroi, K. Tobe and M. Yamaguchi, Phys. Rev. D53 (1996) 2442.

[29] J. Ellis, T. Falk, G. Ganis, K. A. Olive and M. Srednicki, hep-ph/0102098.

[30] ALEPH collaboration, R. Barate *et al.*, Phys. Lett. **B495** (2000) 1 [hep-ex/0011045];
L3 collaboration, M. Acciarri *et al.*, Phys. Lett. **B495** (2000) 18 [hep-ex/0011043];
DELPHI collaboration, P. Abreu *et al.*, Phys. Lett. B **499** (2001) 23;
OPAL collaboration, G. Abbiendi *et al.*, Phys. Lett. **B499** 38.
For a preliminary compilation of the LEP data presented on Nov. 3rd, 2000, see:
P. Igo-Kemenes, for the LEP Higgs working group,
http://lephiggs.web.cern.ch/LEPHIGGS/talks/index.html.